Multi-objective optimization of organic Rankine cycle power systems for waste heat recovery on heavy-duty vehicles

Muhammad Imran[a], Fredrik Haglind[b], Vincent Lemort[c] and Andrea Meroni[d]

[a]Technical University of Denmark, Copenhagen, Denmark, mimran@mek.dtu.dk
[b]Technical University of Denmark, Copenhagen, Denmark, frh@mek.dtu.dk
[c]University of Liege, Liege, Belgium, Vincent.lemort@ulg.ac.be
[d]Technical University of Denmark, Copenhagen, Denmark, andmer@mek.dtu.dk

Abstract:

The use of Organic Rankine Cycle (ORC) power systems for waste heat recovery on internal combustion engines of heavy-duty vehicles can help to mitigate the greenhouse gasses and reduce the fuel consumption of the truck. However, designing an ORC system for this application is a complex process involving trade-offs among factors such as the performance, space/weight restrictions, and cost. This paper presents a multi-objective optimization study of an organic Rankine cycle unit for waste heat recovery from heavy-duty vehicles from techno-economic and sizing perspectives. The optimization was carried out for seven different working fluids using the genetic algorithm to minimize the cost, volume and mass, and maximize the net power output of the ORC unit. The ORC performances for a driving cycle of a truck were also evaluated. In general, the results indicate that the mass, volume, cost and net power output of the ORC system increase with increase in evaporation temperature. The results suggest that when condensation temperature was decreased from 60 °C to 40 °C, the cost, volume, and weight of the ORC unit increased significantly. The maximum net power output, both at design and off-design conditions, is obtained with pentane as working fluid. For this design the net power output of the ORC unit is 10.94 kW at design condition and 8.3 kW at off-design (in average) condition, and the mass, volume, and cost of the ORC system are 129 kg, 1.077 m^3, and 8527 €, respectively.

Keywords:

Waste heat recovery, Organic Rankine Cycle, Internal combustion engine, Multi-objective optimization

1. Introduction

The thermal efficiency of modern internal combustion engines (ICEs) have already reached to their maximum value and only marginal increments are possible [1]. However, still ICEs of heavy duty vehicles convert only approximately 40 % of the combustion heat into mechanical energy, while rest of the heat is rejected to the environment as waste heat [2]. The use of an ORC unit for waste heat recovery on an ICE of heavy-duty vehicles can help to mitigate the greenhouse gasses and reduce the fuel consumption of the truck. However, space limitations, weight, cost, control and off-design performance of the ORC unit, and implications on the ICE performance of the additional back pressure caused by the ORC unit are among the most important aspects that needs to be addressed in order to make the use of ORC power systems for truck applications economically feasible.

The application of the ORC technology to recover exhaust gas heat from heavy duty vehicles was experimentally investigated in number of studies [3-4]. Successfully implemented on a heavy-duty vehicle, an ORC unit is expected to reduce the fuel consumption by 3-10 % [5]. Most of the previous investigations for ORC application for waste heat recovery from ICEs were focused on the cycle configuration, working fluid selection, design and feasibility studies, experimental investigation, dynamic modeling and control, and techno-economic optimization [6].

Several authors suggested that multi-objective optimization and multi-parameters solutions are advisable in order to achieve the best overall thermodynamic and economic performance for ORC power systems [7]. For multi-objective optimization, genetic algorithms (GA) have been extensively adopted for low-grade waste heat recovery problems. Yang et al. [8] developed a thermo-economic model of a dual loop ORC system to analyze both the thermodynamic and economic performance of several working fluid groups for waste heat recovery from a compressed natural gas engine. The net power output per unit heat transfer area and exergy destruction rate were selected as objective functions. The evaporation and condensation pressure were selected as decision variables for the optimization. The optimization was carried out in a GA environment. Their results suggest that at engine maximum rated power point, the ORC system can achieve a maximum net power output per unit heat transfer area of the evaporator of 0.74 kW/m^2, and the ratio of maximum effective heat transfer area to actual area of the evaporator is 69.19 %. Galindo et al. [9] presented a mathematical model of a bottoming ORC coupled to a 2L turbocharged gasoline engine to optimize the cycle from a thermo-economic and sizing point of view using a multi-objective optimization algorithm. The specific volume (ratio of volumetric flow at the outlet of the expander to the power delivered by the expander), specific investment cost, and total area of heat exchangers were used as objective functions. Their results suggest that the optimum value of specific investment cost is 2515 €/kW, area of heat exchangers is 0.48 m^2, and volume coefficient is 2.62 MJ/m^3. Tian et al. [10] carried a techno-economic evaluation of an ORC system used for ICE exhaust gas heat recovery and 20 working fluids were included in the evaluation. The screening criteria was based on the thermal efficiency of ORC, the expansion ratio, the net power output per unit mass flow rate of hot exhaust, the ratio of total heat transfer area to net power output, and electricity production cost. Each fluid was evaluated at the same cycle operating condition. Their results show that R141b, R123 and R245fa give the highest thermal efficiency and net power output values.

Wang et al. [11] performed parametric optimization of a regenerative ORC system for a diesel engine based on particle swarm optimization. The net power output and exergy destruction rate of the regenerative ORC system were selected as the objective functions. The ORC system was optimize for four working fluids and the optimization parameters were evaporating pressure, intermediate pressure, and degree of superheat. The results indicate that the maximum net power output of the ORC system using butane is 36.57 kW, corresponding to an 11 % increase of the diesel engine power output. Hongda et al. [12] performed a multi-objective optimization of a fin-and-tube evaporator for a diesel engine ORC combined system using particle swarm optimization algorithm. Total annual cost, volume of tube bundle, and exhaust pressure drop were considered as optimization objectives, while the geometries of the fin-and-tube evaporator were selected as decision variables. Compared with the results of the original design, the multi-objective optimization resulted in that the volume of tube bundle was increased by 6.5 %, the total annual cost was decreased by 71.5 % and exhaust pressure drop was reduced by 27.6 %.

The literature review indicates that the most commonly employed objective functions in multi-objective optimization studies for ORC for truck applications are the total investment cost, net power, area of heat exchangers, thermal efficiency and exergy efficiency. However, an optimization of the mass and volume of the ORC system is not yet reported. Due to the weight and volume restrictions on trucks, it is much more important to address the mass and volume of the ORC unit used for trucks than for many other applications. This paper presents a multi-objective optimization study of an organic Rankine cycle unit for waste heat recovery from heavy-duty vehicles from techno-economic and sizing perspectives. The optimization was carried out for seven different working fluids using the genetic algorithm to minimize the cost, volume and weight and maximize the net power output of the ORC unit. In addition, the ORC performances for a driving cycle of a real truck were evaluated. The preliminary design of the ORC system was based on a 0D model, which was extended to 1D-component models. The mass, volume and cost of the ORC system were calculated using empirical correlations.

2. System Description

The waste heat is recovered from the exhaust gas of a 450 hp diesel engine of a long-haul truck. It is 13 L Euro 6 engine with Selective Catalytic Reduction (SCR); Exhaust Gas Recirculation (EGR) is not used. A schematic of the waste heat recovery system is shown in Fig. 1.

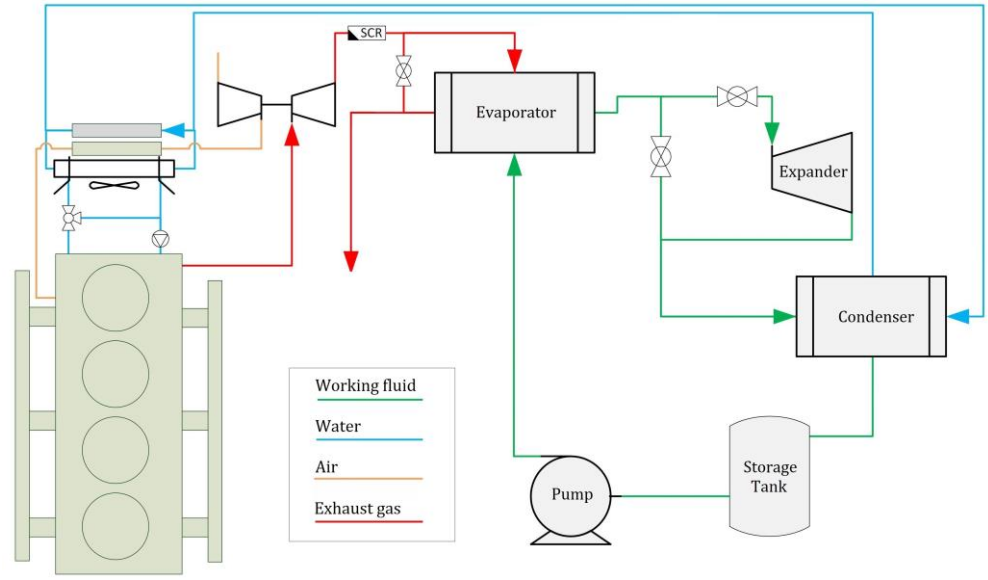

Fig. 1. Schematic of the organic Rankine cycle unit for waste heat recovery from the ICE

The heat from the ORC condenser can be rejected using the existing engine radiator or an additional radiator dedicated to the ORC unit. Therefore, the optimization was performed for two condensation temperatures, 40 °C, assuming that an additional radiator is used, and 60 °C, assuming that the existing engine radiator is used. In order to achieve an optimal design considering the operational cycle of the truck/engine, the conditions for which the ORC unit are designed play a significant role. In the present study, the heat source conditions corresponding to 40 % engine load were selected as the design point of the cycle. The design point was selected based on experiences shared by a truck manufacturer. The operating conditions of the engine in the design point are shown in Table 1 (the data were provided by the truck manufacturer).

Table 1. Engine data at engine operating conditions 40 % engine load

Engine		Exhaust gas conditions (after SCR)	
Speed (RPM)	Power (kW)	Flow rate (kg/h)	Temperature (°C)
1200	148	897	317

Based on the aforementioned assumptions two cases were defined:

- Case 1 for condensation temperature of 40 °C
- Case 2 for condensation temperature of 60 °C

The initial screening of working fluids was based on the global safety criteria, environmental impact, and thermodynamic characteristics. The global safety factor is summarized in one single factor based on the NFPA 704 system [13]:

$$GSF = \alpha * H + \beta * I + \gamma * F \quad (1)$$

H, I and F are health, instability and flammability values as per NFPA 704, and α, β and γ are weightage factors for each safety factor. The major importance has been given to the flammability factor (α =50 %), while medium importance was given for the instability factor (β =35 %) and lowest importance was given for the health hazard (γ =20 %).

The working fluids with global safety value of higher than 2.5 and low global warming potential and ozone depletion potential (<1) were selected for the optimization. Further, fluids that will be phase out in 2020 and 2030 were removed from the list of candidate working fluid. Finally, seven working fluids were selected for optimization as shown in Table 2.

Table 2. Properties of the selected working fluids for the optimization

Working fluids Name	Molar mass (kg/kmol)	Normal boiling point (°C)	Critical temperature (°C)	Critical pressure (bar)	NFPA 704 Classification H	F	R	GWP 100 yrs	ODP
Ethanol	46	79	242	41	0	3	0	NA	0
MDM	237	153	291	14	0	2	0	NA	0
MM	162	100	246	19	1	4	0	NA	0
Pentane	72	36	197	34	1	4	0	7	0
R1233zd(E)	131	18	166	36	2	0	0	1	0.0003
R245fa	134	15	154	37	2	1	0	1030	0
RE347mcc	200	34	165	25	3	0	0	530	0

3. System Modeling

3.1. Sizing of the ORC system

The evaporator and condenser are brazed plate heat exchanger and were selected due to their compact size. The evaporator and condenser design models are based on one-dimensional discretization in the flow direction, assuming equidistant steps of enthalpy rate change for both the fluids. Heat transfer and pressure drop in each control element were calculated by solving the heat transfer and fluid flow conditions for each control volume. The temperatures for heat transfer calculations were estimated at the control volume center points, interpolating the values between the nodes. .

The inlet and outlet conditions (temperature and mass flow rate) of primary and secondary fluid was taken as input from the cycle design. For a selected heat exchanger geometry, the model is initiated with an assumed number of plates. The design algorithm is iterative and calculates the required number of plates that satisfy the required heat load and pressure drop restriction. In order to minimize the effect of the ORC on the ICE performance, a 30 kPa pressure drop limitation was implemented in exhaust side of the evaporator. Appropriate correlations were used for the flow boiling of the working fluid [14], condensation of the working fluid [15], cooling water [16], and exhaust gas [17]. The heat exchanger design algorithm was validated against our previous work [7] and Unisim [18] (a commercial heat exchanger design software). The results of the validation indicate that for the same plate geometry and working conditions, the difference in the number of the plates predicted by the models is less than 4 %.

The pump is characterized by its isentropic efficiency, which is assumed constant with a value of 65 %. An in-house model of a radial-inflow turbine written in the MATLAB language was used to perform the preliminary design of the expander. For given specifications from the thermodynamic cycle (i.e., mass flow rate, inlet temperature, pressure and stage pressure ratio) and a set of decision variables related to the turbine geometry, the model solves the governing equations for mass, energy and momentum in the main turbine stations, and estimates the preliminary design and isentropic total-to-static efficiency of the machine. The turbine design model has been validated with a number of test cases from the open literature, and showed an accuracy in the turbine isentropic efficiency within ± 3 %-points

3.2. Economic model

The cost of the system was divided into direct cost and indirect cost. The cost of the system components, installation, working fluid, piping, and instrumentation and control are included in direct cost, while the engineering and contingency costs are included in indirect cost. The business model approach is adopted to estimate the cost of the ORC system [19]:

$$TCS = DC + IC \quad (2)$$

$$DC = C_{sys} + C_{wf} + C_{pipe} + C_{inst,ctr} + C_{inst} \quad (3)$$

$$C_{sys} = C_{pp} + C_{hx,eva} + C_{hx,con} + C_{exp} \quad (4)$$

$$C_{pipe} = 0.15\, C_{sys} \quad ; \quad C_{inst,ctr} = 0.2\, C_{sys} \quad ; \quad C_{inst} = 0.3\, C_{sys} \quad (5)$$

$$IC = C_{eng} + C_{cont} \quad ; \quad C_{eng} = 0.08\, DC \quad ; \quad C_{cont} = 0.15\, C_{eng} \quad (6)$$

From a business point of view, a production of 20000 units per year was assumed. The costs of the expansion machine and heat exchangers were estimated using the costing add-in function in Solidworks software [19]. The cost of the ORC components is shown in Table 3. Comparisons with figures supplied by equipment suppliers indicate that the cost estimation method used here is reasonable.

Table 3. Cost correlations for the ORC components [20]

Component	Dependent variable	Cost (€)
Expander	Rotor diameter (m)	$C_{exp} = 164338 d_4^{2.08}$
Pump	Consumed power (W)	$C_{pp} = 150 \times \left(\dot{W}_p / 300\right)^{0.25}$
Heat exchanger	Metal mass (kg)	$C_{hx} = 250 + 5 M_{hx}$

3.3. Mass and volume

The total mass of the ORC system consists of the mass of ORC components, mass of piping, mass of the instrumentation/control system. An additional mass of 10 % is added to the total mass to account for the mass of the storage tank, and other auxiliary components [21]:

$$\mathrm{TM} = 1.1 * (M_{sys} + M_{pipe} + M_{inst,ctr}) \quad (7)$$

$$M_{sys} = M_{pp} + M_{hx,eva} + M_{hx,con} + M_{exp} + M_{wf} \quad (8)$$

$$M_{pipe} = 0.14\, M_{sys} \ [21] \quad ; \quad M_{inst,ctr} = 0.02\, M_{sys} \ [21] \quad (9)$$

The volume of the ORC unit was calculated by adding the volume of all the individual components:

$$TV = V_{sys} + V_{aux} \quad ; \quad V_{sys} = V_{pp} + V_{hx,eva} + V_{hx,con} + V_{exp} \quad ; \quad V_{aux} = 0.3\, V_{sys} \quad (10)$$

The volume of piping network, tank, and instrumentation (V_{exp}: auxiliary components) was taken as 30 % of the volume of the ORC components. The mass and volume of the components were based on input and suggestions provided by suppliers/manufacturers. These data were used to develop polynomial fits for mass and volume of the expander, pump and heat exchangers. The mass and volume correlations for ORC components are shown in Table 4. The mass and volume correlations of the expander are based on expander power (kW), while for pump the correlations are based on the differential pressure (bar) across the pump. Expander correlations are valid for a turbine size from 5 kw to 25 kW. The pump is positive displacement pump and correlations are valid for a differential pressure from 5 to 20 bar. The heat exchanger correlations are valid for chevron type brazed plate heat exchanger. For further details, readers are referred to [22–24].

Table 4. Correlation for the estimation of mass and volume of the ORC system [22–24]

Component	Correlation
Expander mass (kg)	$M_{exp} = 0.0455\left(W_{exp}\right)^2 - 0.0968\,W_{exp} + 11.43$
Expander volume (m^3)	$V_{exp} = -0.00001\left(W_{exp}\right)^2 + 0.0018\,W_{exp} + 0.0027$
Heat exchanger mass (kg)	$M_{hx} = M_{conn} + N_{pl}\,M_{pl}$
Heat exchanger volume (m^3)	$V_{hx} = L_{pl} + WD_{pl}\left[N_{pl}\left(t_{pl} + S_{pl}\right)\right]$
Pump mass (kg)	$M_{pp} = 0.0049\left(\Delta P_{pp}\right)^2 + 0.637\,\Delta P_{pp} + 5.2$
Pump volume (m^3)	$V_{pp} = 0.000008\left(\Delta P_{pp}\right)^2 + 0.0012\Delta P_{pp} + 0.0021$

Industry data along with the results of the correlations for weight and mass of the expander are shown in Fig. 2.

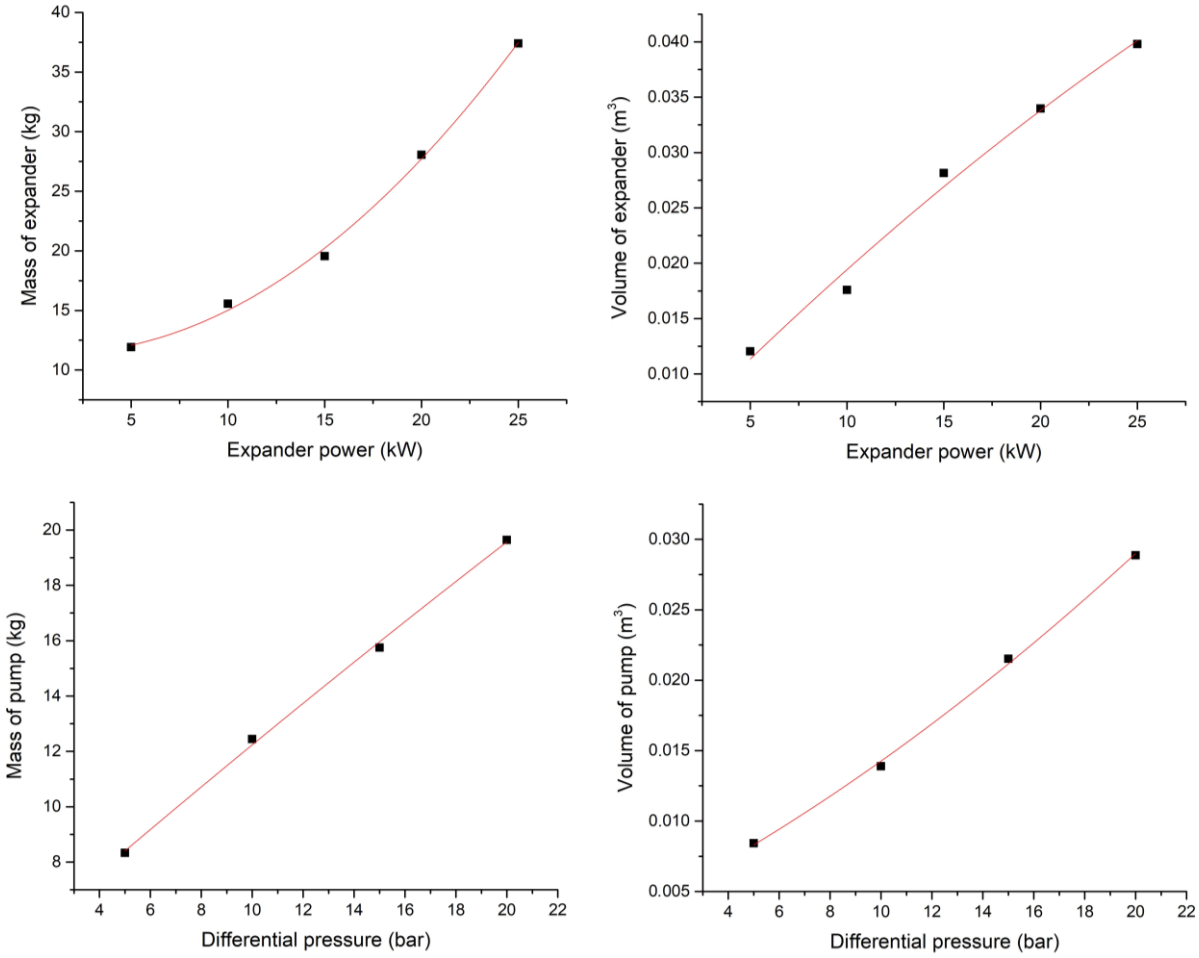

Fig. 2. Mass and volume plot of the expander. The curves represent the correlations listed in Table 4, while the dots indicate data supplied by manufacturers/suppliers.

3.4. Optimization

The optimization of the ORC system was carried out by using the genetic algorithm. The detailed layout of the optimization approach is shown in Fig. 3.

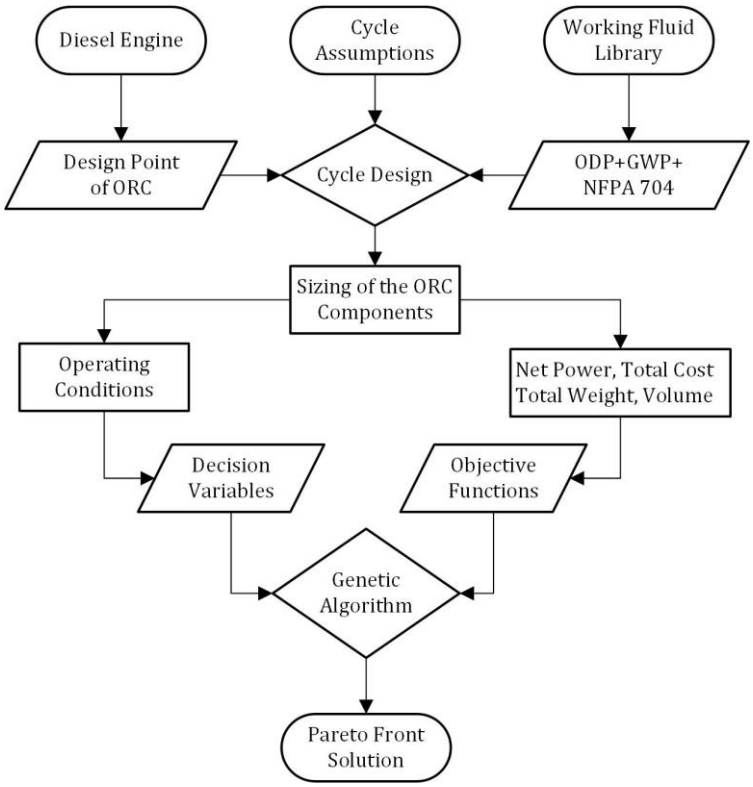

Fig. 3. Flow chart of the optimization approach

3.4. Off-design model of ORC

In order to evaluate the performance of the ORC along the operational profile of the diesel engine, an off-design model was implemented. The inputs for the model are the exhaust gas temperature and mass flow rate values from real driving conditions of a diesel engine of a long-haul truck. During the off-design simulations, the control strategy was based on the sliding evaporator pressure, keeping the condenser pressure constant, and controlling the working fluid mass flow rate.

The performance variation of the heat exchangers, where one fluid was a gas or vapor, were modeled based on variations in the overall UA value of the heat exchangers. In these heat exchangers, the gas or vapor side is assumed to dominate the heat transfer processes resulting in a UA value variation governed by the gas or vapor mass flow rate. The UA value and pressure losses in the heat exchangers at off-design were assumed to vary according to the following function [25-26]

$$(UA)_{od} = (UA)_{ds}\left[\frac{\dot{m}_{od}}{\dot{m}_{ds}}\right]^{0.6} \quad ; \quad (\Delta P)_{ofd} = (\Delta P)_{ds}\left[\frac{\dot{m}_{od}}{\dot{m}_{ds}}\right]^{2} \tag{11}$$

As for the pump, its efficiency in off-design conditions was approximated with a third degree polynomial including the ratio of the inlet volumetric flow at off-design condition to that at design condition [27]:

$$\left(\eta_{pp}\right)_{od} = \left(\eta_{pp}\right)_{ds}\left\{-0.029265\left[\frac{\dot{V}_{od}}{\dot{V}_{ds}}\right]^{3} - 0.14086\left[\frac{\dot{V}_{od}}{\dot{V}_{ds}}\right]^{2} + 0.3090\left[\frac{\dot{V}_{od}}{\dot{V}_{ds}}\right] + 0.8638\right\} \tag{12}$$

$\dot{V}$ is the volume flow rate at the pump inlet and $\left(\eta_{pp}\right)_{ds}$ is the pump design efficiency. In order to evaluate the turbine performance in off-design conditions, a swallowing capacity model based on Beckmann's equation was used [28]. The Beckmann's equation, determines the mass flow rate at the turbine inlet as a function of the evaporator pressure, the fluid specific volume at the turbine outlet and the turbine size:

$$\dot{m}_{wf} = \left[C_{T,B} + K(\mu - \mu_{ds})\right](1+\mu)\sqrt{\frac{P_{exp,i}F}{V_{exp,i}\mu}} \quad ; \quad C_{T,B} = \frac{\dot{m}_{wf}\sqrt{T_{exp,i}}}{\sqrt{\left({P_{exp,i}}^2 - {P_{exp,o}}^2\right)}} \tag{13}$$

3.5. Optimization

A multi-objective optimization was carried out using the Genetic Algorithm involving both thermodynamic and economic performances. The following objective functions and variables were employed:

$$\begin{aligned} F_1(x) &= Maximize\,[Wn] = Maximize\left[\frac{\dot{W}_{exp} - \dot{W}_{pp}}{Q_{eva}}\right] \\ F_2(x) &= Minimize\,[TM] = Minimize\left[1.1 * (M_{sys} + M_{pipe} + M_{inst,ctr})\right] \\ F_3(x) &= Minimize\,[TV] = Minimize\left[1.3 * \left(V_{pp} + V_{hx,eva} + V_{hx,con} + V_{exp}\right)\right] \\ F_4(x) &= Minimize\,[TCS] = Minimize\,[DC + IC] \end{aligned} \tag{14}$$

Decision variables and their lower and upper bounds:

$50\ °C \leq$ Evaporation temperature $\leq 0.9 *$ Tcr & $0\ °C \leq$ Superheat at turbine inlet $\leq 50\ °C$

$5\ °C \leq$ Pinch point temperature difference in the evaporator $\leq 20\ °C$

During the optimization, component geometry, and other cycle parameters were kept constant and the objective functions were evaluated by varying the decision variables.

4. Results and discussion

4.1. Optimization

The aim of a multi-objective optimization study is to find the Pareto frontier optimal solution. Each point of the frontier represents one potential solution in the multi-objective optimization problem. The selection of the final optimum depends on the importance of each objective. A single value of decision variables cannot satisfy all the objective functions simultaneously. The result of optimization study for pentane for a condensation temperature of 40 °C is shown in Fig. 4.

Table 5. The optimized designs providing the highest net power output of the ORC system

Case	Working fluid	Objective functions				Decision variables		
		Wn (kW)	TM (kg)	TV (m^3)	TCS (€)	Teva (°C)	SH (°C)	PPTDeva (°C)
1	Pentane	10.94	129	1.07	8527	167	12	13
	Ethanol	9.97	134	1.18	4054	191	13	12
	R1233zd(E)	9.68	122	0.93	6275	137	6	10
	MM	9.51	128	0.97	5118	196	3	11
	MDM	9.08	130	1.12	4455	205	4	9
	R245fa	8.94	118	0.84	5156	130	7	14
	RE347mcc	8.49	116	0.79	4361	139	15	16
2	Pentane	8.53	113	0.939	4552	173	8	10
	Ethanol	7.51	112	0.25	2470	197	11	10
	MM	7.45	109	0.36	3032	206	6	10
	R1233zd(E)	7.19	108	0.83	3296	142	8	9
	MDM	7.08	109	0.25	2714	217	7	8
	R245fa	6.48	105	0.83	2778	135	11	11
	RE347mcc	6.34	102	0.62	2581	144	12	14

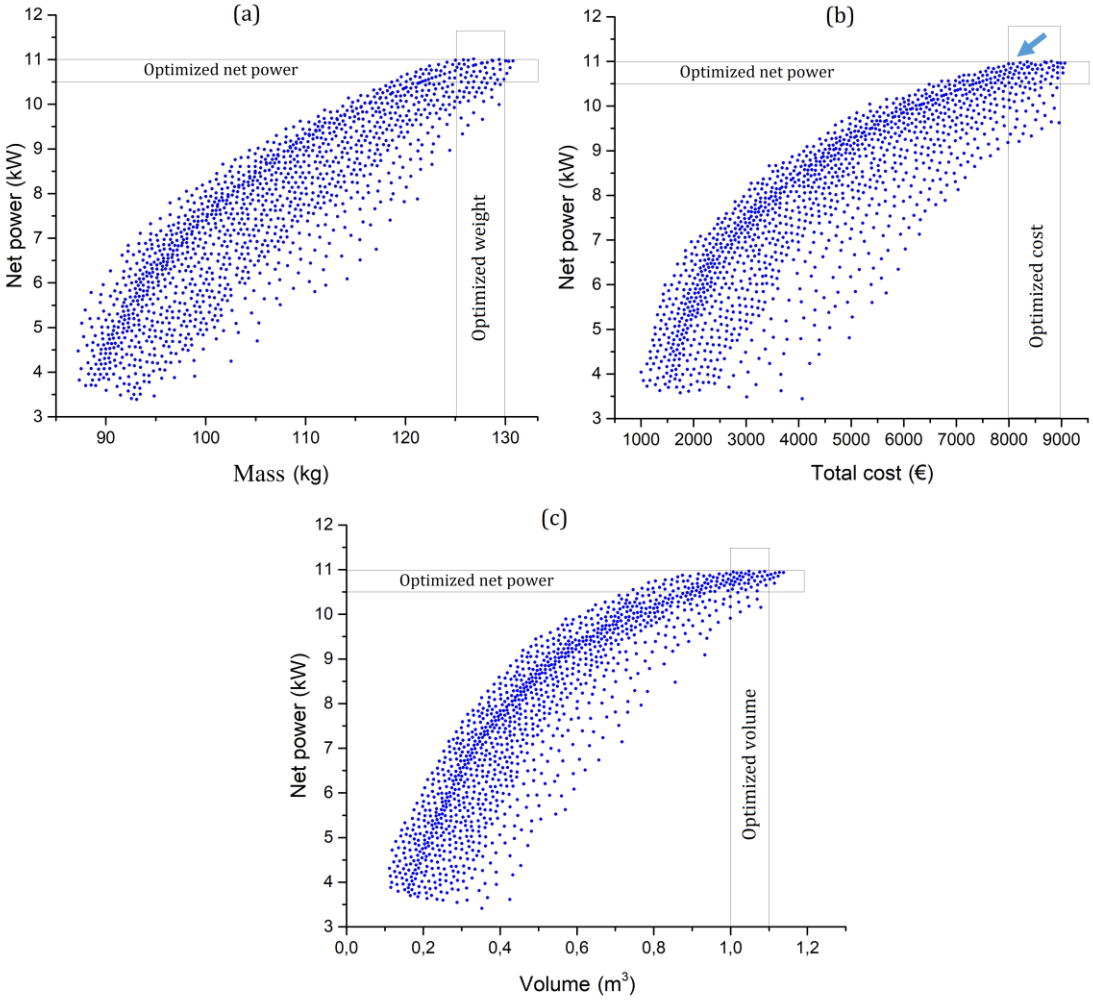

Fig. 4. Pareto front of a) net power vs mass, b) net power vs total cost, and c) net power vs volume of ORC system for pentane (condensation temperature of 40 ℃)

From the Pareto front trend, it is clear that an increase in net power result in increases in the values of cost, weight and volume. The maximum net power area is highlighted in a rectangle as optimized power; the corresponding values of the weight, volume and cost are also highlighted in rectangles as shown in Fig. 4. The maximum value of the net power corresponding to minimum cost of the ORC system was selected as the optimized design, see the arrow in Fig. 4b. For each working fluid, the values of objective function corresponding to optimized net power and decision variables are shown in Table 5. The results indicate that the optimized net power is higher in case 1 than in case 2. This can be explained by temperature difference between the heat source and heat sink. The higher temperature difference between heat and sink, the higher will be the net power. However, the higher temperature difference also results in the increase in volume, weight and cost of the system. Each working fluid corresponds to different values of the optimized objective functions. The highest net power was achieved for pentane and the lowest was achieved for RE347mcc.

The variation of the net power output, cost, volume and weight for the ORC system for pentane is shown in Fig. 5. The evaporation temperature has a higher influence on the objective function than other decision variables of the optimization. The values of each objective function increases with the increase in evaporation temperature due to the increase in size of the individual components of the ORC system. A significant increase in the values of each objective functions is observed at an evaporation temperature of 120 °C and above. It may be observed that when the condensation temperature is decreased from 60 °C to 40 °C, the net power, weight, cost and volume of ORC unit is increased by 22 %, 12.2 %, 46 %, and 12 % respectively.

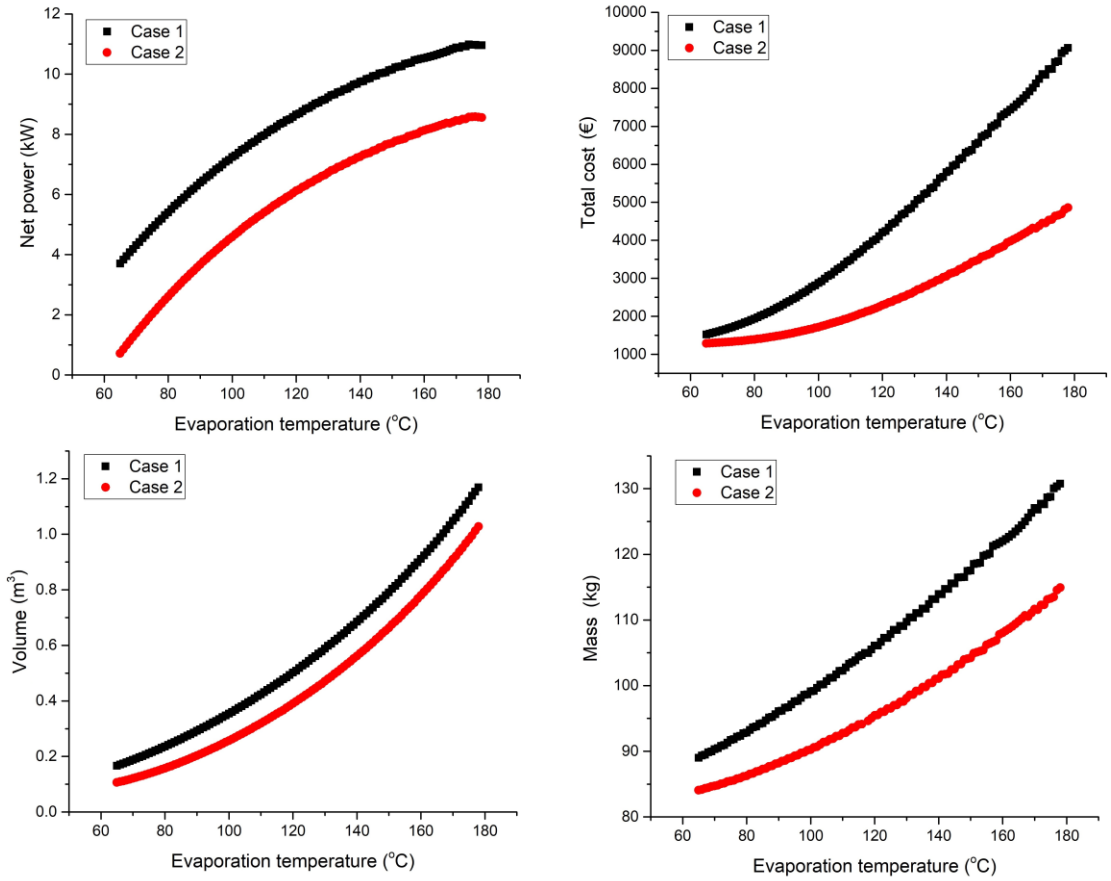

Fig. 5. Variation of the net power output, weight, volume, and total cost of ORC system with evaporation temperature of pentane (Case 1: Tcon = 40 ℃, Case 2: Tcon = 60 ℃)

4.2. Off-design performance assessment

Data in terms of mass flow rate and temperature of the engine exhaust gases after the SCR (see Fig. 1) for a real driving cycle was provided by a truck manufacturer (including 2700 data points in total), shown in Fig. 6. The data was split into 'bins', discretized over an 8x7 grid, representing groups of data of similar quantities in order to reduce the computational effort of the off-design model. Each bin was assigned mass flow rate and temperature values equal to the values at the center of each bin. Furthermore, each bin was assigned a histogram weighting based upon the number of data points contained within the bin. For the off-design performance, the design condition of the system corresponding to the optimized values of the objective functions, shown in Table 4, were used. The average net power output in off-design conditions was calculated by weighting the value for each bin based on the number of points within each bin (representing how often a given condition occurs). For cases 1 and 2, the ORC unit operates 40 % of the time at heat source conditions lower than its design value. The difference between the net power in design and off-design condition was highest for MDM. It was mainly due to lower isentropic efficiency of MDM turbine at part-load conditions. The lowest variation of the net power was observed for R1233zd. The off-design results obtained using the bin approach were also compared with the approach considering all 2700 data points. The relative deviation in results between two methods is less than 1 %. However, the compilation time for the approach including all data is 17 hours, while the same simulation is performed in 43 minutes using the bin approach.

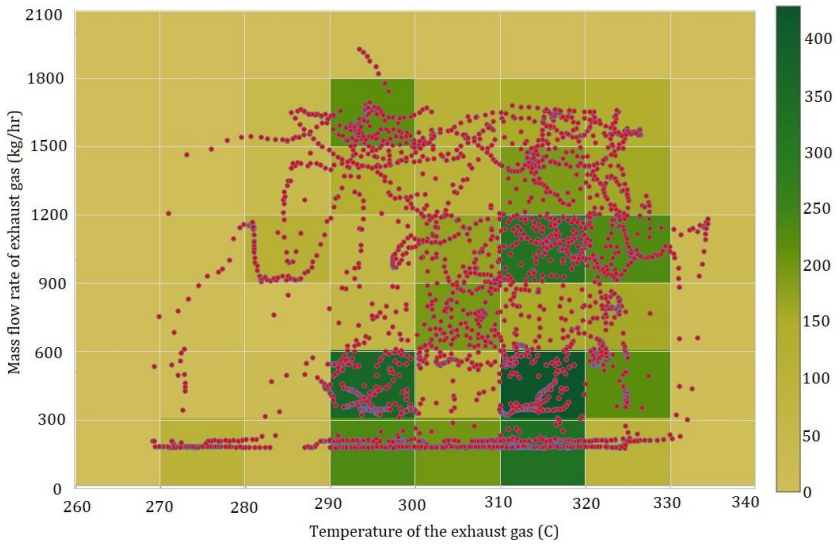

Fig. 6. Mass flow rate and temperature of the exhaust gases after the SCR for a real driving cycle.

Table 6. Average net power output of the ORC unit at design and off-design conditions

Case 1			Case 2		
Working fluid	Net power (kW)		Working fluid	Net power (kW)	
	Off-design	design		Off-design	design
Pentane	8.31	10.94	Pentane	7.04	8.53
R1233zd	7.55	9.68	R1233zd	6.04	7.19
Ethanol	7.08	9.97	Ethanol	5.92	7.51
R245fa	6.62	8.94	MM	5.71	7.45
RE347mcc	6.54	8.49	R245fa	5.25	6.48
MM	6.47	9.51	RE347mcc	5.28	6.34
MDM	5.81	9.08	MDM	5.22	7.08

For case 1 with pentane as working fluid, which is the design providing the highest net power output at design conditions, the variation of the net power output of the ORC unit with exhaust gas heat condition is shown in Fig. 7. The temperature of the exhaust gas after the SCR does not vary significantly during the driving cycle, while there is a significant variation of the exhaust mass flow rate with the engine load. During accelerating and deaccelerating periods, the power produced by the ORC unit is lower than 1 kW due to very low mass flow rate of the exhaust gas.

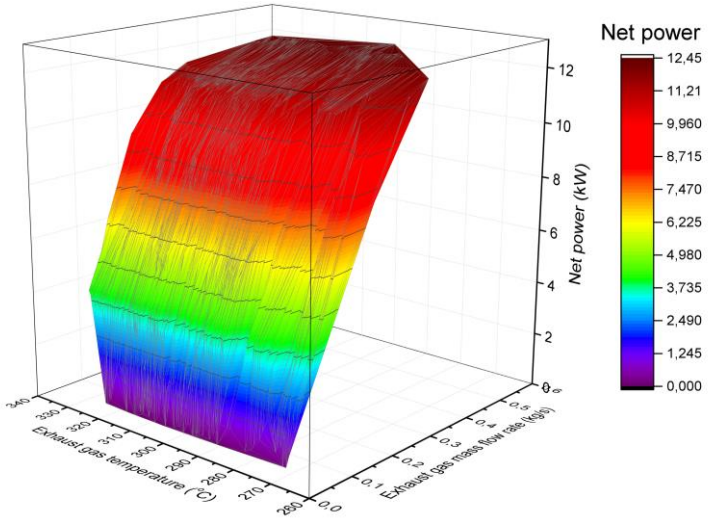

Fig. 7. Part-load map of net power output for Case 1 with pentane as working fluid

5. Conclusions

A multi-objective optimization model of an ORC system was developed to analyze both the thermodynamic and the economic performances of several working fluids for the purpose of waste heat recovery from the exhaust gas of a diesel engine of a heavy-duty vehicle. The genetic algorithm was employed to obtain the Pareto optimal solutions from the viewpoints of maximizing the net power output and minimizing the cost, weight and volume of the ORC system. The off-design performance of a real driving cycle was evaluated for the ORC systems. In general, the results indicate that the weight, volume, cost and net power output of the ORC system increase with increase in evaporation temperature. Moreover, as expected, the net power output of the ORC unit is higher when designed with a condensation temperature of 40 °C than designed with a condensation temperature of 60 °C. The maximum net power output, both in design and off-design conditions, is obtained for pentane as working fluid. For this design the net power output of the ORC unit is 10.93 kW/8.3 kW in design/off-design (average) conditions, and the weight, volume, and cost of the ORC system are 129 kg, 1.077 m^3, and 8527 €, respectively . When the condensation temperature is decreased from 60 °C to 40 °C, the net power, weight, cost and volume of ORC unit with pentane as working fluid increased by 22 %, 12.2 %, 46 %, and 12 % respectively.

Acknowedgement

The research presented in this paper has been funded by the European Union's Horizon 2020 research and innovation programme with a Marie Skłodowska-Curie Individual Fellowship under grant agreement no. 751947 (project DYNCON-ORC). The financial support is gratefully acknowledged.

Nomenclature

C	Cost, €	N	Number	W	Power, kW
DC	direct cost, €	$\dot{m}$	Mass flow rate, kg/s	P	Pressure, bar
IC	indirect cost, €	TCS	The cost of the system, €	t	Plate thickness, m
L	Length, m	TV	Total volume of system, m^3	S	Plate spacing, m
V	Volume, m^3	TW	Total mass of system, kg	T	Temperature, °C
M	Mass, kg	WD	Width of plate, m	η	Efficiency

Subscripts and superscripts

con	Condenser	eng	Engineering	od	Off design point
$cont$	Contingency	exp	Expander	pp	Pump
$conn$	Connection	eva	Evaporator	sys	System
ds	Design point	hx	Heat exchanger	wf	Working fluid

References

[1] S. Lion, C. N. Michos, I. Vlaskos, C. Rouaud, and R. Taccani, "A review of waste heat recovery and Organic Rankine Cycles (ORC) in on-off highway vehicle Heavy Duty Diesel Engine applications," *Renew. Sustain. Energy Rev.*, vol. 79, pp. 691–708, 2017.

[2] A. Domingues, H. Santos, and M. Costa, "Analysis of vehicle exhaust waste heat recovery potential using a Rankine cycle," *Energy*, vol. 49, no. 1, pp. 71–85, 2013.

[3] Y.-Q. Zhang *et al.*, "Development and experimental study on organic Rankine cycle system with single-screw expander for waste heat recovery from exhaust of diesel engine," *Energy*, vol. 77, pp. 499–508, 2014.

[4] J. F. Oudkerk, R. Dickes, O. Dumont, and V. Lemort, "Experimental performance of a piston expander in a small- scale organic Rankine cycle," *IOP Conf. Ser. Mater. Sci. Eng.*, vol. 90, p. 12066, 2015.

[5] T. A. Horst, W. Tegethoff, P. Eilts, and J. Koehler, “Prediction of dynamic Rankine Cycle waste heat recovery performance and fuel saving potential in passenger car applications considering interactions with vehicles’ energy management,” *Energy Convers. Manag.*, vol. 78, pp. 438–451, 2014.
[6] M. Imran, F. Haglind, M. Asim, and J. Zeb Alvi, “Recent research trends in organic Rankine cycle technology: A bibliometric approach,” *Renew. Sustain. Energy Rev.*, vol. 81, 2018.
[7] M. Usman, M. Imran, Y. Yang, D. H. Lee, and B.-S. Park, “Thermo-economic comparison of air-cooled and cooling tower based Organic Rankine Cycle (ORC) with R245fa and R1233zde as candidate working fluids for different geographical climate conditions,” *Energy*, vol. 123, 2017.
[8] F. Yang, H. Zhang, C. Bei, S. Song, and E. Wang, “Parametric optimization and performance analysis of ORC (organic Rankine cycle) for diesel engine waste heat recovery with a fin-and-tube evaporator,” *Energy*, vol. 91, pp. 128–141, 2015.
[9] J. Galindo, H. Climent, V. Dolz, and L. Royo-Pascual, “Multi-objective optimization of a bottoming Organic Rankine Cycle (ORC) of gasoline engine using swash-plate expander,” *Energy Convers. Manag.*, vol. 126, pp. 1054–1065, 2016.
[10] H. Tian, G. Shu, H. Wei, X. Liang, and L. Liu, “Fluids and parameters optimization for the organic Rankine cycles (ORCs) used in exhaust heat recovery of Internal Combustion Engine (ICE),” *Energy*, vol. 47, no. 1, pp. 125–136, 2012.
[11] H. Wang *et al.*, “Parametric optimization of regenerative organic rankine cycle system for diesel engine based on particle swarm optimization,” *Energies*, vol. 8, no. 9, pp. 9751–9776, 2015.
[12] H. Liu, H. Zhang, F. Yang, X. Hou, F. Yu, and S. Song, “Multi-objective optimization of fin-and-tube evaporator for a diesel engine-organic Rankine cycle (ORC) combined system using particle swarm optimization algorithm,” *Energy Convers. Manag.*, vol. 151, no. September, pp. 147–157, 2017.
[13] S. Amicabile, J. I. Lee, and D. Kum, “A comprehensive design methodology of organic Rankine cycles for the waste heat recovery of automotive heavy-duty diesel engines,” *Appl. Therm. Eng.*, vol. 87, pp. 574–585, 2015.
[14] M. Imran, M. Usman, Y. Yang, and B.-S. Park, “Flow boiling of R245fa in the brazed plate heat exchanger: Thermal and hydraulic performance assessment,” *Int. J. Heat Mass Transf.*, vol. 110, 2017.
[15] Y.-Y. Yan and T.-F. Lin, “Condensation heat transfer and pressure drop of refrigerant R-134a in a small pipe,” *Int. J. Heat Mass Transf.*, vol. 42, no. 4, pp. 697–708, Feb. 1999.
[16] H. Martin, “A theoretical approach to predict the performance of chevron-type plate heat exchangers,” *Chem. Eng. Process. Process Intensif.*, vol. 35, no. 4, pp. 301–310, Jan. 1996.
[17] J. Yang, A. Jacobi, and W. Liu, “Heat transfer correlations for single-phase flow in plate heat exchangers based on experimental data,” *Appl. Therm. Eng.*, vol. 113, pp. 1547–1557, 2017.
[18] “UniSim – Software for Process Design and Simulation.” [Online]. Available: https://www.honeywellprocess.com/en-US/explore/products/advanced-applications/unisim/Pages/default.aspx. [Accessed: 09-Jan-2018].
[19] L. Guillaume, “On the design of waste heat recovery organic Rankine cycle systems for engines of long-haul trucks. PhD Thesis,” University of Liege, 2017.
[20] L. Guillaume, A. Legros, R. Dickes, and V. Lemort, “Thermo-Economic Optimization of Organic Rankine Cycle Systems for Waste Heat Recovery From Exhaust and Recirculated Gases of Heavy Duty,” in *VTMS 13 - Vehicle Thermal Management Systems Conference*, 2017, pp. 109–125.
[21] R. Daccord, “Cost to benefit ratio of an exhaust heat recovery system on a long haul truck,” *Energy Procedia*, vol. 129, pp. 740–745, 2017.
[22] “Brazed plate heat exchangers.” [Online]. Available: https://www.alfalaval.com/products/heat-transfer/plate-heat-exchangers/Brazed-plate-heat-exchangers/. [Accessed: 15-Jan-2018].
[23] “Green Energy Turbine.” [Online]. Available: https://deprag.com/en/green-energy/green-energy-turbine/. [Accessed: 10-Dec-2017].
[24] “T Series Pumps.” [Online]. Available: https://www.tuthillpump.com/index.cfm/products/productdetail/?p=56&ps=36. [Accessed: 13-Jan-2018].
[25] S. Lecompte, H. Huisseune, M. van den Broek, S. De Schampheleire, and M. De Paepe, “Part load based thermo-economic optimization of the Organic Rankine Cycle (ORC) applied to a combined heat and power (CHP) system,” Elsevier, Nov. 2013.
[26] J. G. Andreasen, A. Meroni, and F. Haglind, “A comparison of organic and steam Rankine cycle power systems for waste heat recovery on large ships,” *Energies*, vol. 10, no. 4, pp. 1–23, 2017.
[27] J. P. Veres, “Centrifugal and axial pump design and off-design performance prediction,” *NASA Techincal Memo. 106745*, pp. 1–24, 1994.
[28] M. E. Mondejar, F. Ahlgren, M. Thern, and M. Genrup, “Quasi-steady state simulation of an organic Rankine cycle for waste heat recovery in a passenger vessel,” *Appl. Energy*, vol. 185, pp. 1324–1335, 2017.